Return to Session

VERIFICATION OF MECHANICAL SUPPORT FOR CABLES USED ON BRIDGE STRUCTURES AT DILATION POINTS

Vincent Rouillard, Victoria University (Australia) Vincent.Rouillard@vu.edu.au
Roman Piechota, Olex (Australia) rpiechot@olex.com.au
Graeme Barnewall, Olex (Australia) gbarnewa@olex.com.au
Ken Barber, Olex (Australia) kbarber@olex.com.au

ABSTRACT

This paper describes a series of experiments developed to evaluate the mechanical performance of a cable-supporting transition structure designed to accommodate bridge structure dilation. A full size prototype of the bow spring structure was commissioned and a series of experiments were undertaken to study the mechanical behaviour of the structure. In addition to generating essential data for validating the design of the structure, the experiments yielded valuable results relating to the mechanical behaviour of the structure as well as the effects of dilation on the mechanical integrity of the cable.

KEYWORDS

Transition structure, dilation, cable, curvature.

INTRODUCTION

One of the most significant challenges for cable performance and reliability is where there is a change of condition. Examples are where cables are jointed and terminated, transferred from direct buried to in-duct, from in-air to in-ground, horizontal to vertical etc. One of the most difficult conditions is often where cable might be subjected to additional forces such as bridge structure dilation. In such cases, the uniqueness of the structure calls for a unique solution. In the case presented here, the original bridge design did not include the possibility of additional loads to be carried by the installation of cables onto the structure. A special steel structure, to support a double circuit with 1600mm² 132kV XLPE cables across the entire span of the bridge, was designed to be suspended from the bridge.

At the bridge expansion points where bridge dilation occurs, a structure was specially designed as a pair of pin-jointed curved beams. In order to validate various design criteria, as well as to better understand the mechanical behaviour of such a unique structure, a series of original experiments were designed and undertaken. The experiments were aimed at investigating the effects of dilation on the forces and bending moments generated within the structure as well as the forces transmitted to the bridge structure under a range of conditions were studied. The effect of repeated applications of full extension-contraction cycles, representing deformations due to annual extremes in temperature, to the structure and the cables was investigated. In addition, the flexural characteristics of the cable were investigated and the paper shows how cable curvature was used to estimate the bending strains and stresses within the cable.

Finally, experiments aimed at characterising the vibratory behaviour of the transition structure as well as recommending and validating a practical and effective vibration mitigation strategy.

EXPERIMENTAL ARRANGEMENT

A full size prototype of the transition structure (fig. 1) was commissioned to experimentally validate the design analysis. Two specially designed frames were fabricated to provide a rigid support for each extremity of the bow spring. One frame (located at the dead end of the loading frame) was firmly anchored to the laboratory's concrete floor and the other (located at the live end of the loading frame) was

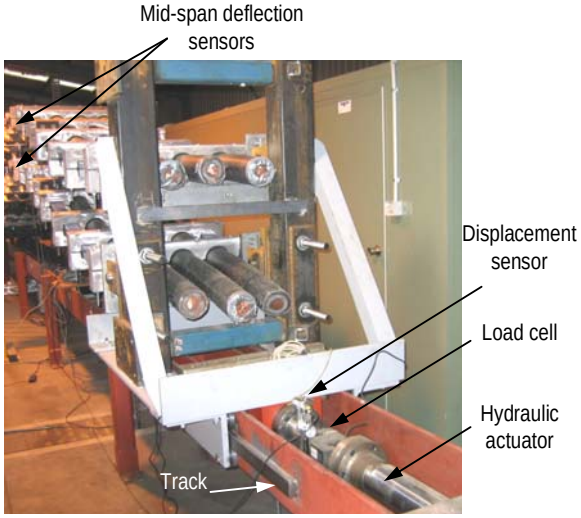

Figure 1: Prototype and test rig.

mounted on low-friction tracks and connected to a hydraulic actuator via a force sensor. Both frames were designed so as not to deflect more than 0.5 mm at full load. This was verified experimentally using dial gauges which indicated deflections inferior to 0.3 mm (longitudinally and laterally) at a height corresponding to the load axis of the bow spring. Longitudinal deformation simulating dilation was applied using the hydraulic actuator.

The prototype transition structure and the supporting frame were fitted with an array of strain gauges and displacement sensors in order to determine their mechanical behaviour under simulated dilatation of the bridge structure (fig. 2).

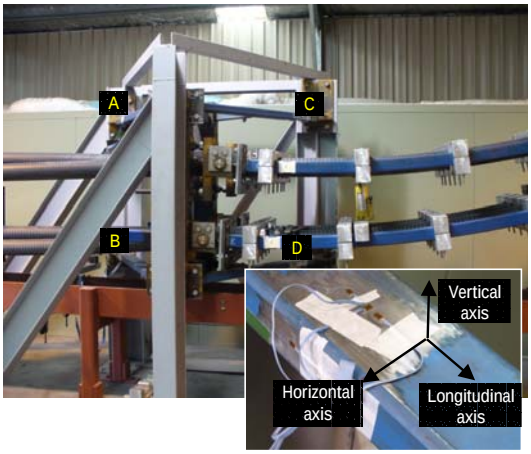

Figure 2: Strain gauges at four locations on supports.

RESULTS

Bow spring stiffness

The effects of dilation on the forces and bending moments generated within the structure as well as the forces transmitted to the bridge structure under a range of conditions were studied. The change in force, mid-span deflection and strains in the bow spring was evaluated when longitudinal deformation, replicating expected dilation due to annual ambient thermal variations (45.4 mm contraction and 25.4 mm extension) was applied.

Results from these experiments, shown in figs. 3 & 4, revealed that the forces transmitted onto the bridge structure as well as the longitudinal and bending strains along the length of the bow spring structure generally matched those predicted by numerical analysis

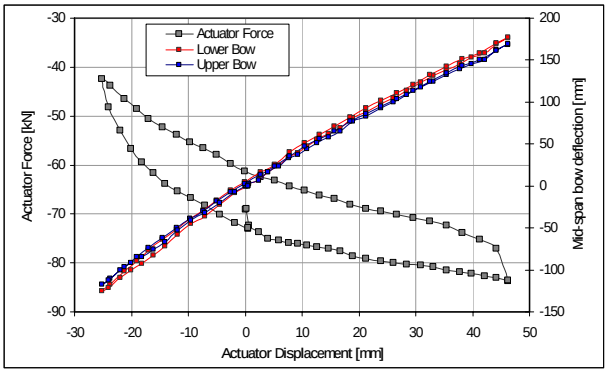

Figure 3: Typical results showing actuator force and mid-span deflections vs dilation.

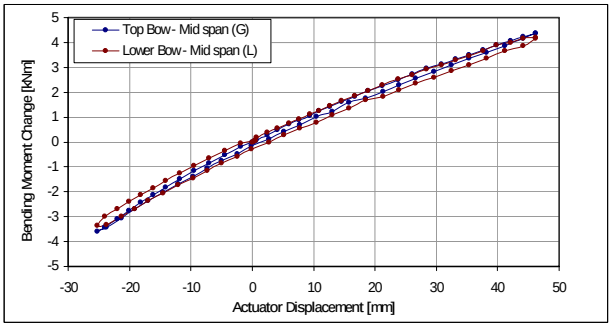

Figure 4: Typical results showing bending moments variations caused by dilation.

Bow spring endurance

Given that the design life of the structure is 50 years, it was deemed important to undertake an experiment with the aim of establishing the endurance characteristics of the assembly. An experiment was designed to determine whether repeated applications of variations in curvature expected to be experienced by the cable and the bow spring under normal service conditions have any significant effect on the mechanical integrity of the cable and the bow spring assembly. This was achieved by subjecting the prototype assembly, comprising the bow spring and all six cables, to 100 repetitive cyclic deflections of the most severe expected dilation (45.4 mm contraction and 25.4 mm extension) representing 100 years' service. The mechanical integrity of the assembly was evaluated by monitoring the overall stiffness of the structure throughout the test as well as by regular visual observations. The assembly's stiffness was established by monitoring the relationship between the longitudinal force required to contract and deflect the structure and the resulting deflection of the bow springs at mid-span.

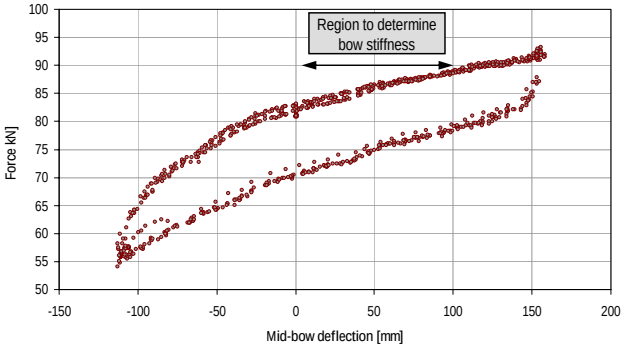

Figure 5: Force-deflection data for 100 dilation cycles.

The results of the endurance experiment are displayed in fig. 5 where the force – deflection data for every 10 contraction / extension cycle of the bow spring assembly are shown. The stiffness of each bow was established by computing the line of best fit through the force deflection data lying between 0 and 100 mm on the contraction part of the stroke. The results show that the stiffness of the structure remained generally constant throughout the test which indicates that the structural integrity of the assembly was retained. This finding was confirmed by careful inspection of both the bow spring structure and the cables therein, which did not exhibit any evidence of damage.

Cable curvature and strain

Inherent to the design of the transition structure is the fact that the cables are bowed to follow the curved shape of the bow spring and, as the bow spring changes its shape due to dilation, so do the cables. This change is reflected in a variation in the cables' curvature. It is this recurring change in curvature and its effect on the mechanical integrity of the cables that were addressed in a series of experiments designed to:

- o determine the variation of the curvature of the cable due to dilation of the bow spring.
- o evaluate the change in strain in the outer layer of the cable due to variations in curvature.
- o determine whether there exists significant curvature and movement of the cable relative to the trefoil clamps (fig.

6) due to thermal expansion of the bow spring.

- Determine the flexural characteristics of the cable including force - curvature relationships as well as force – strain relationships.

Figure 6: Cable layout on bow spring.

Curvature was established by measuring the height of the cable above a reference plane at regular intervals along the bow using a calibrated measuring tape while the cable movement relative to the trefoil clamp and curvature over the first "snake" was measured using dial gauges. In addition, estimates of the variation in bending strain, at specific locations on the outer (upper) layer of the cable due to changes in curvature, were estimated. This was achieved by placing strain gauges at regular intervals along the top of the central cable on the lower bow. This was done while the bow was in its neutral position. The cable curvature and strain were evaluated with the bow spring at its neutral position as well as full contraction (45.4 mm) and full extension (25.4 mm). The vertical position of the cable at regular intervals of 0.5 m for the three main bow spring positions are shown in fig. 8 in which the position of the bow spring pin and the first trefoil clamp are also shown. Cable curvature was computed by first evaluating a cubic spline functions for each set of data (also shown in fig. 7) in order to accommodate for the relatively large horizontal interval of 0.5 m. The curvature radius was then computed by determining the radius of the circle of best fit fitting through three adjacent horizontal – vertical coordinates for the entire test length. These are shown in fig. 8 which reveals that the most severe curvature (smallest curvature radius) occurs at the crest of the bow and reaches a value of 4 m when the bow is fully contracted. Curvature radii of approximately 5 m occur at 1.5, 2.0 and 3.0 m from the bow crest. It must also be noted that curvature in the region of the bow spring pin connection is not significant compared to the most severe curvature along the cable. The results also show that the cable undergoes a variation in curvature radius of 1.6 m (4 to 5.6 m) at the bow crest for each thermal expansion cycle.

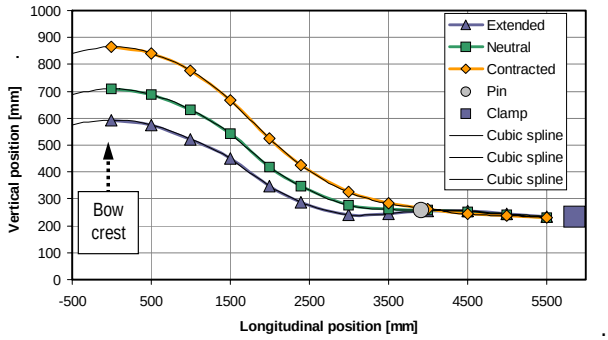

Figure 7: Cable shape for various dilation values.

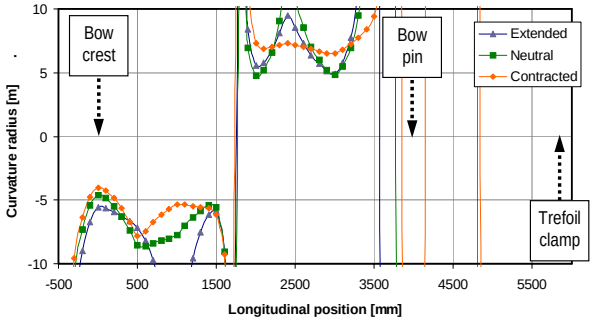

Figure 8: Cable curvature radius due to dilation.

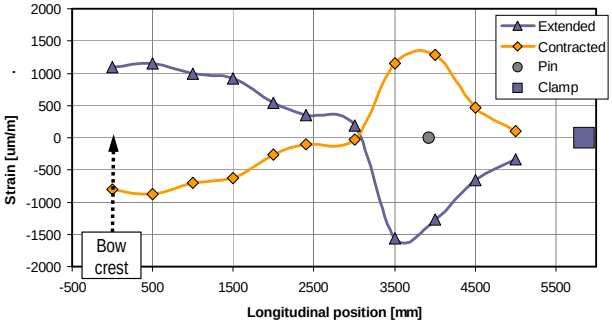

Figure 9: Variations in cable strain due to dilation.

The variation in bending strain along the cable due the contraction and extension of the bow spring is shown in fig. 9. It can be seen that the change in bending strain generally decreases as the distance away from the bow crest increases, there is a sharp rise at 3.5 m near the bow spring pin support. This is attributed to the fact that the cables are firmly secured together at the trefoil clamps which provide additional restriction of movement in the longitudinal direction. The effect of these variations in bending strain on the mechanical integrity of the cable will be addressed in the following section.

Cable flexural characteristics

The flexural characteristics of the cable were evaluated using a three-point bending test configuration in order to simulate changes in curvature induced to the cable by the contraction and extension of the bow spring. The specific aims of this series of experiments were to determine the flexural characteristics of the cable to establish relationships between the applied force, cable curvature and bending (curvature) strain, to determine whether the in-service cable curvature is significant and to establish whether repeated applications of curvature variations have a detrimental effect on the mechanical integrity of the cable.

The experiments were carried out on a programmable universal testing machine equipped with a precision force transducer and an extensometer. In addition, the mechanical strain on the outer layer of the cable due to variations in curvature was evaluated by placing a strain gauge on the underside of the cable sample near the mid-span. Cable curvature was estimated from the mid-span deflection data by first determining the relationship between mid-span deflection and curvature represented by an empirical formula (shown in fig. 10).

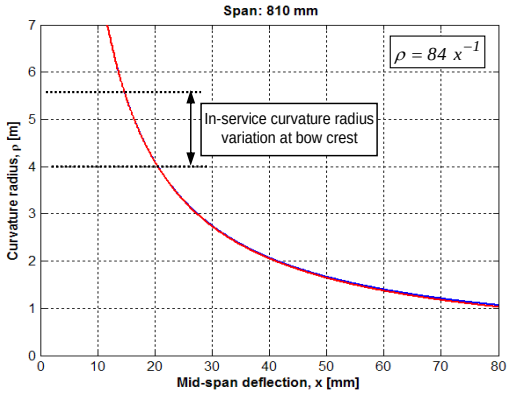

Figure 10: Relationship between mid-span deflection and curvature radius.

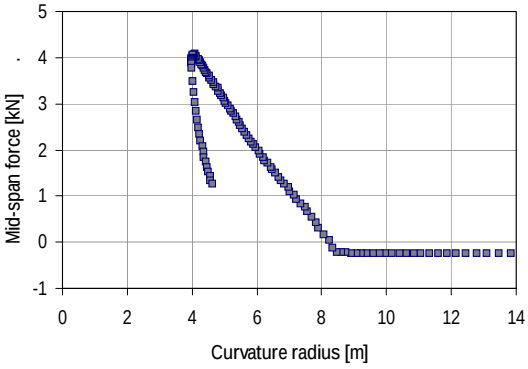

Figure 11: Flexural characteristics of XLPE cable.

The flexural characteristics of the cable were first evaluated by subjecting the cable sample to a mid-span deflection equivalent to the maximum expected curvature (4.0 m) as established. This was applied to a number of samples all of which were found to conform to the typical characteristics shown in fig. 11 which indicates a significant level of flexural hysteresis in the cable.

The curvature limit of the cable was evaluated by applying mid-span deflections of increasing amplitudes with the cable sample placed in a three-point bending configuration. The results, shown in fig. 13, reveal that the cable is able to withstand curvatures significantly more severe that those expected to be sustained by while in service. Fig. 12 shows that the inherent flexural stiffness of the cable (slope of the force – deflection curve) remains largely unchanged as the load cycle magnitude increases which is a reliable indication that the mechanical integrity of the cable is not adversely affected. This outcome was confirmed by visual observation of the cable samples which failed to reveal any significant damage.

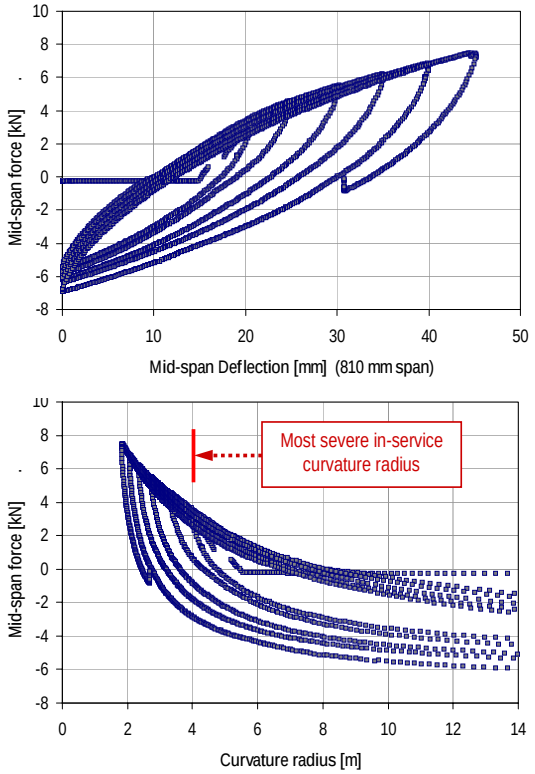

Figure 12: Flexural characteristics of XLPE cable for various curvature values.

The effect of repeated applications of curvature variations on the mechanical integrity of the cable was evaluated by applying mid-span deflection cycles equivalent to curvature radii of 4.0 – 5.6 m which were measured at the crest of the bow. The deformation cycles were applied at a rate of 72 cycles per hour (50 seconds per cycle) while the mid-span force, deflection and strain were continuously recorded. The results of the experiments are shown in fig. 13 which shows that the basic flexural characteristics of the cable sample remain largely unchanged with repeated applications of curvature fluctuations.

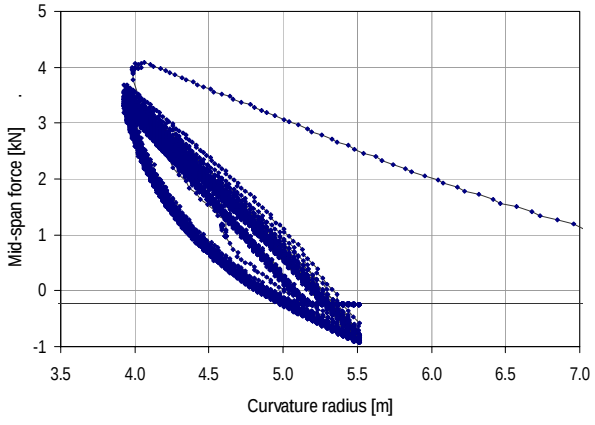

Figure 13: Flexural characteristics of XLPE cable for repeated applications of deformation cycles.

One noticeable feature of the results is the reduction in the force required to achieve the pre-determined curvature. Further analysis of the collected data (fig. 14) reveals the nature of the decay which is due to stress relaxation of the cable. Although this decay may imply some “flexural

softening" of the cable, it is, in fact, attributed to the small indentations made to the cable outer layers by the supports used in the three-point bending apparatus. The unchanged flexural stiffness is a more reliable indicator that the cable's mechanical integrity remained essentially unaffected by the repeated applications of curvature variations. Careful inspection of the cable samples, subjected to repeated applications of curvature variations, did not show any observable signs of mechanical damage.

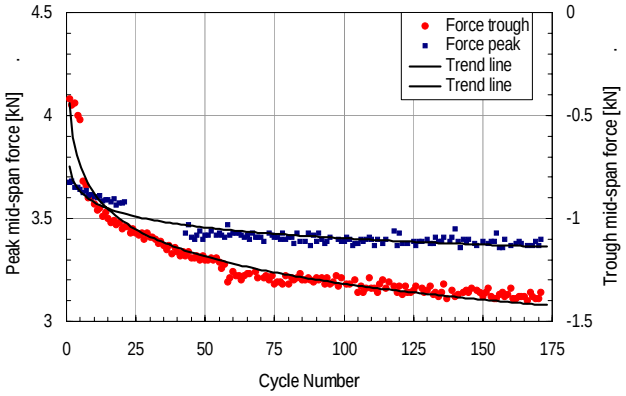

Figure 14: Mid-span force relaxation on XLPE cable for repeated applications of deformation cycles.

Fig. 15 shows the relationship between cable curvature and the variation in surface strain at mid-span of the cable sample set in a three-point bending configuration for repeated application of curvature cycles. The results reveal a strong correlation between curvature and surface strain. It is also interesting to note that the amplitude in strain variation (approx. 3,300 micro strain) in bending is similar to that measured from the cable on the prototype assembly (approx 3,900 micro strain). This is a strong indication that the cable is capable of sustaining numerous applications of curvature variations without suffering significant changes in it mechanical integrity.

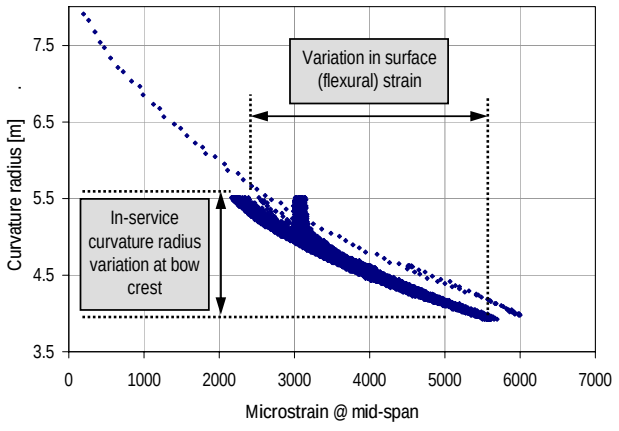

Figure 15: XLPE strain vs curvature radius.

Vibration damping

Because of the inherent spring-like compliant nature of the bow springs, each structure has a propensity to vibrate at its natural frequencies when disturbed. Experiments were undertaken to establish whether these natural vibrations are expected to be excessive under normal operating conditions and to make recommendations on mitigation strategies to minimise the amplitude of these vibrations without affecting the functionality of the bow spring. The study included a survey of the nature and levels of background vibrations on the host bridge under normal operating conditions which was found to be random and of very low levels (less than 0.05 g rms). The resonant characteristics of the structure as well as the corresponding level of self-damping were evaluated experimentally by inducing suitably large mechanical disturbances (forceful agitation) to the structure and measuring the resulting vibrations with a high sensitivity piezoelectric accelerometer. The recorded decaying vibrations were analysed to establish the vibratory behaviour of the bow springs, namely, the resonant frequencies and the corresponding mode shapes, and equivalent viscous damping ratios. This was achieved by computing the frequency spectrum of the signal (fig. 16) as well as the logarithmic decrement (using the Hilbert Transform) of the vibration signal band-pass-filtered around the resonant frequency of interest (fig. 17).

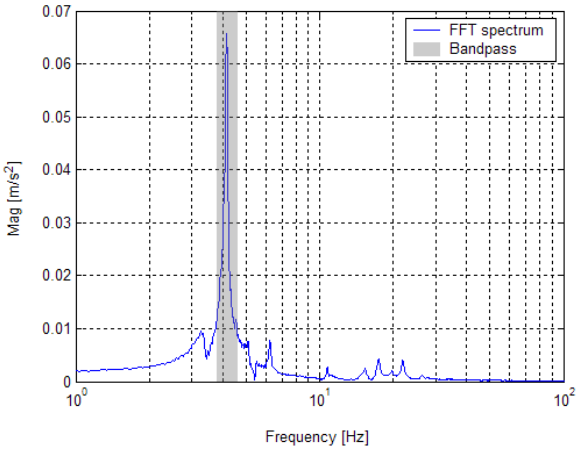

Figure 16: Typical frequency spectrum of bow spring vibrations.

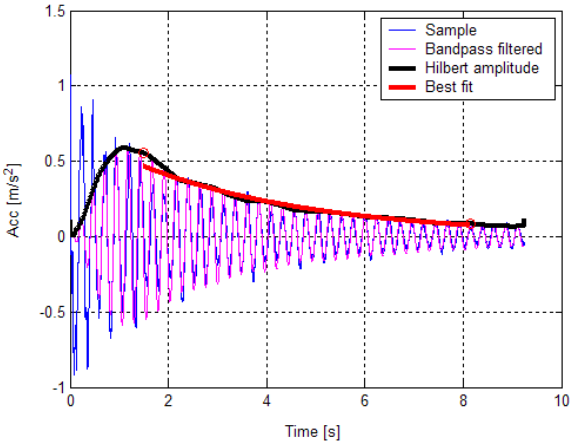

Figure 17: Illustration of decaying vibrations along with logarithmic decrement envelope.

Results yielded from the self-damping experiments show that the structure is very lightly damped and exhibits resonances in the vertical and lateral planes at relatively low frequencies which are likely to generate significant vibratory deflections given sufficiently severe disturbances. This suggests that additional damping is required to limit the vibratory deflections should the bow springs experience resonance. The level of supplementary damping to the

structure was ultimately determined by the maximum allowable force transmitted to the supporting structure namely the bridge. Supplementary damping needed to be applied to the most prominent vibration modes namely the bending modes in the vertical and lateral planes. Supplementary damping is governed by the damping coefficient, c:

$$c = \zeta c_c = 2\zeta m\omega_n \quad [1]$$

where ζ is the damping ratio, c_c is the critical damping of the structure, m is the modal mass of the structure and ω_n is the undamped natural frequency of the structure. For each bow spring the lineal density has been estimated at around 150 kg/m and the natural frequency of the first mode was established at around 4 Hz. Given the boundary condition of the bow spring, the modal mass can be approximated at 600 kg (half the total mass). This produces the following relationship:

$$c \approx 31{,}000\zeta \quad Nsm^{-1} \quad [2]$$

The force, F_t , transmitted to the supporting structure via a viscous damper is given by,

$$F_t = cv = 31{,}000\zeta d\omega_n\sqrt{1-\zeta^2} \quad N \quad [3]$$

where d is the expected amplitude of vibration and v is the vibratory velocity at the resonant frequency. This relationship is shown in fig. 18 for various levels of vibration amplitudes and reveals that, even at relatively high damping ratios ($\zeta >$ 0.3), the estimated peak transmitted force is not excessive as long as the vibration amplitude is small (less than 4 mm).

After careful consideration, a number of hydraulic (viscous) dampers rated at 3,400 Nsm^{-1} were attached to each bow spring as shown in fig. 19.

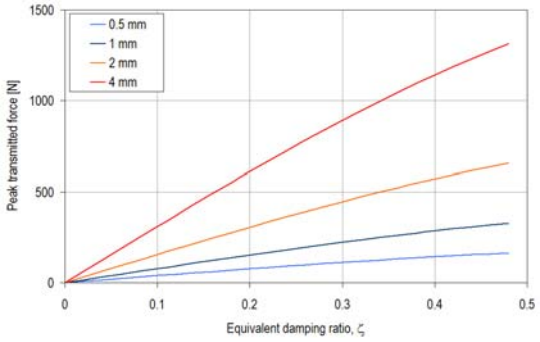

Figure 18: Resonant force vs damping ratio for various vibratory amplitudes.

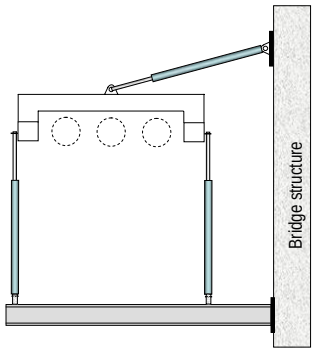

Figure 19: Hydraulic damper configuration.

The effectiveness of the dampers was evaluated by experimentally quantifying the increase in damping of the structure as well as to estimate the peak forces that are likely to be transmitted to the supporting bridge structure via the
dampers. Figure 20 shows vibration records obtained with and without dampers fitted to the bow spring. The main effect of the dampers is revealed by the accelerated rate at which the vibrations decay as well as an overall reduction in the amplitude of vibration. Overall, the introduction of dampers to the structure resulted in an increase in equivalent viscous damping from 1.4 % to 10% while the maximum force transmitted through each damper due to vibration was estimated at less than 500 N.

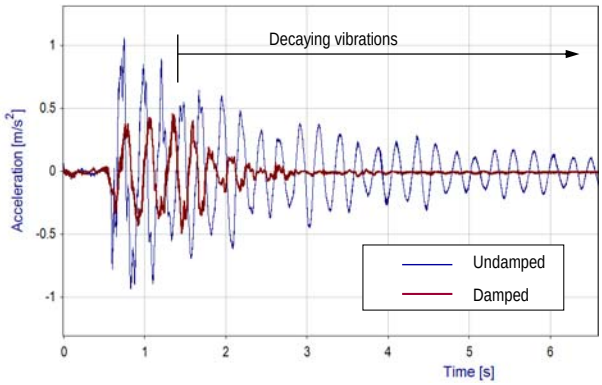

Figure 20: Effect of dampers on the decaying bow spring vibrations.

CONCLUSION

The paper has presented the development of a number of unique experiments the results of which were used to validate the mechanical behaviour of the transition structure against various design criteria. Results show that the forces transmitted onto the bridge structure as well as the longitudinal and bending strains along the length of the bow spring structure generally matched those predicted by numerical analysis. Importantly, the experiments yielded valuable data pertaining to the flexural behaviour of the cables when subjected to variations in curvature. The paper also describes the approach used to reduce the severity of vibrations within the structure and demonstrates the effectiveness of introducing viscous dampers to the structure. The work presented here clearly demonstrates the value of carrying-out carefully thought-out experiments on unique transition structure designs. Results generated by this work have enhanced our understanding of the structure's behaviour and will, no doubt, be of great value when designing similar transition structures in the future.

REFERENCES

[1] C.M. Harris, 1996, *Shock and Vibration Handbook,* McGraw-Hill, NY, USA, 37.1-37.23.

GLOSSARY

RMS: Root-mean-square